

Figure 2.23 Impedance graphs of ionic liquid BDMI-TFSI (pink), BDMI-TFSI and expanded graphite (red) and BDMI-TFSI and commercial graphene (green).

### **Chapter3. GRAPHENE OXIDE REDUCTION METHODS**

In this chapter three of the most low cost, green and safe methods for the reduction of the graphene oxide are presented and discussed. Starting from a brief introduction on the most common reduction techniques reported in literature, the results obtained investigating three different methods of reduction for the graphene oxide by using chemical, UV-light and hydrothermal techniques, considered reliable, easy, low cost and environmentally friendly will be characterized and compared. All the characterizations performed in order to have a qualitative and quantitative analysis on the actual reduction of the material and about the removal of the functional groups on the surface of the graphene oxide are also reported and discussed in detail.

#### **3.1 Reduction Methods Overview**

Top-down synthesis techniques, compared to bottom-up, involve one more step for the preparation of the final material: the reduction of the functional groups present on the graphene oxide surface. In fact, the bottom-up techniques, as discussed in Chapter 2, produce monolayers of carbon atoms with a very low amount of defects and functional groups if compared to the top-down processes. The reason for this difference can be addressed to the synthesis process. As discussed in Chapter 2, in contrast to pristine graphite, the graphite oxide (graphene oxide sheets, GO) are heavily oxygenated, bearing hydroxyl and epoxide functional groups on their basal planes, in addition to carbonyl and carboxyl groups located at the sheet edges (104), (105). The presence of these functional groups makes GO sheets strongly hydrophilic, which allows them to readily swell and disperse in water (99). Previous studies have shown that a mild ultrasonic treatment of graphite oxide in water results in its exfoliation to form stable

aqueous dispersions that consist almost entirely of one-nm-thick sheets (106). Due to their structure, GO sheets are not electrically conductive. Therefore, an additional step is needed to reduce the oxide to graphene.

A second step in the graphene production, that consists in the exfoliation of the graphite oxide, introduces even more defects in the atomic structure (87) due to the mechanical shearing among the flakes due to the sonication process they are subject to. Graphene oxide has, on the positive side, excellent water solubility properties and very homogeneous water dispersions can be achieved employing a short sonication time (88) without the use of surfactants. The conductivity values instead, are much lower compared to the ones of the pristine graphene and for this reason the graphene oxide is generally subjected to a reduction process to lower the number of the functional groups and to restore higher conductivity values (89).

The reduction of GO, a process that restores the original structure and properties of graphene, can be achieved by several methods, e.g., by thermal (107), chemical (108), (90), (53), or photo-thermal (109), (110) treatments. By far the most common chemical reducing agent used for the reduction of the graphene oxide is the hydrazine hydrate, a very hazardous and toxic material usually employed in the Hummers method. It is reported that the reduced graphene oxide obtained by the effect of the hydrazine, exhibits high electronic conductivity values (91). Although hydrazine is the most common reducing agent used to prepare reduced graphene oxide, high toxicity and hazardous bi-products greatly limit its use for the large-scale preparation of graphene for industrial applications.

Graphene oxide can be also reduced applying significant temperature with a fast heating rate during chemical reaction (92). The key concerns of the graphene community regarding the reduction process used, remain the one of achieving the highest reduction capability, healing the defective graphene oxide, be able to selectively by removing a single type of oxygen group, improving the dispersion stability of the resulting graphene, as well as applying environmentally friendly and affordable reducing agents that are also the principle at the base of this investigations proposed in the next sessions of this chapter.

## 3.2 Experimental Session: Reduction of the Graphene Oxide

In this section it is first presented the analysis performed on commercial graphene oxide, used as a starting material for all the experiments reported in this chapter. The reduction studies done through the use of three different reducing techniques, with the goal of obtaining a more conductive material, possibly spendable for electronic applications will be then presented. The reduction techniques investigated had the goal of involving environmentally friendly material and processes, abundant and cheap materials and easy manufacturing. The three different approaches for the reduction of the graphene oxide investigated in this dissertation are i) the chemical reduction, through the dispersion of the graphene oxide in water based of sodium silicate solution, ii) UV-light reduction (93) with a catalytic effect provided by the introduction of a photo initiator and iii) hydrothermal reduction (94), as reducing method of water based graphene oxide solution in autoclave with a moderate temperature. The results and the characterizations are going to be presented and discussed in the following sections.

**Characterization of the Commercial Graphene Oxide** In order to compare the results obtained from the three reducing processes examined, the starting material was analyzed with several morphological and compositional characterization techniques. The commercial graphene oxide was purchased from ACS Materials and came in a powder that was then dispersed in water with a concentration of 0.5 mg/ml and sonicated in a bath sonicator for 30 minutes. The dispersion was then drop cast onto a silicon wafer with an oxide layer 300 nm thick. In Figure 3.1 it is possible to see an optical microscope image of the graphene oxide deposited on the silicon wafer. The different colors are produced by the different refraction of the light due to the different thickness of the graphene oxide flakes.

The shape of the flakes is irregular and the average size is about 10  $\mu\text{m}$ , as confirmed also by FE-SEM analysis reported in Figure 3.1 c. Raman spectroscopy was also performed and the spectrum is showed in Figure 3.1 b, which confirms the carbon nature of the flakes by showing the typical G peak at 1595  $\text{cm}^{-1}$ , the disorder D peak at 1344  $\text{cm}^{-1}$  and the 2D peak 2691  $\text{cm}^{-1}$  (86).

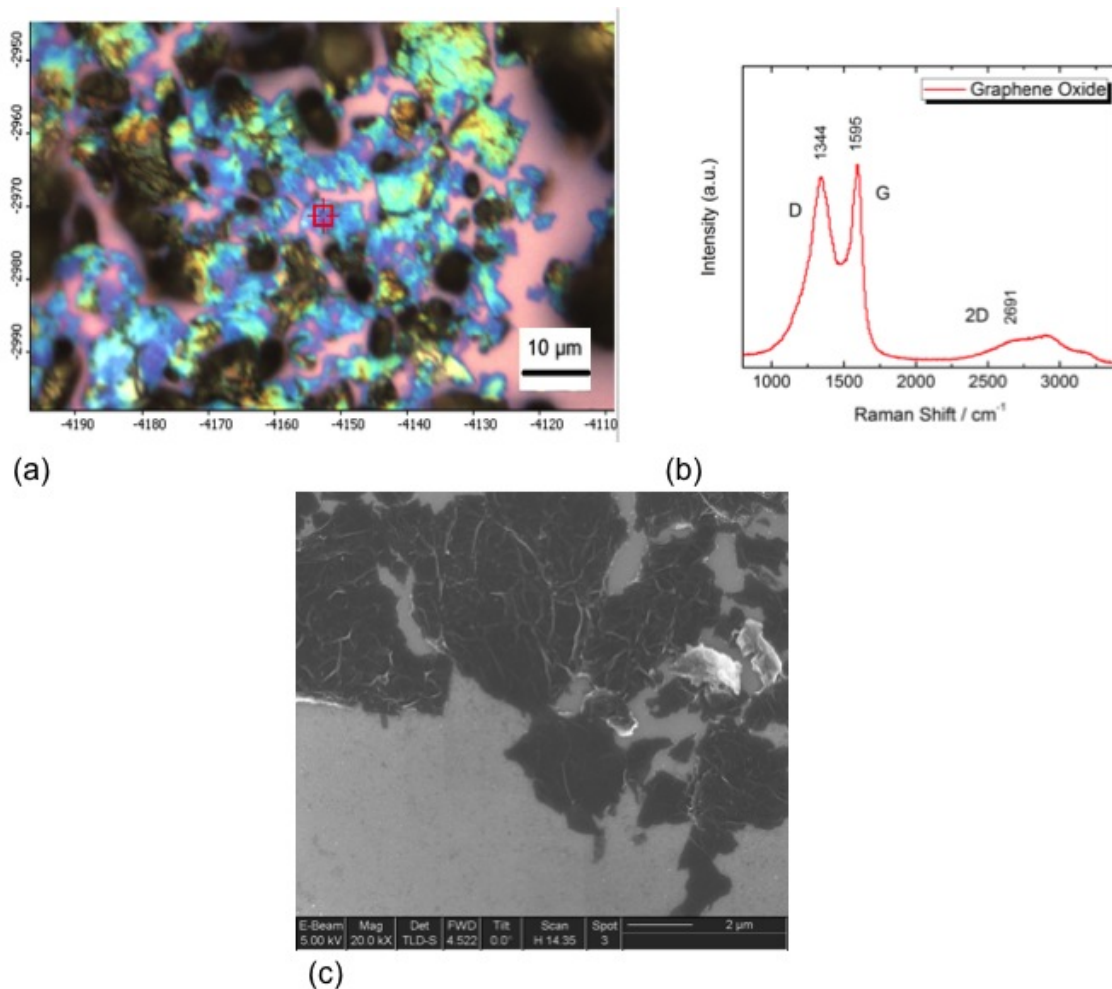


Figure 3.1 Optical picture (a), Raman spectrum (b) and SEM picture (c) of commercial graphene oxide deposited on a 300 nm silica oxide wafer.

The XRD analysis has also been performed and as it is reported in Figure 3.2, a peak is present at 11.6 degree, giving an important information on the inter layers distance, calculated from the Bragg's law ( $n\lambda = 2d\sin\theta$ , where  $n$  is an integer,  $\lambda$  is the incident wavelength,  $d$  is the spacing between the planes in the atomic lattice, and  $\theta$  is the angle between the incident ray and the scattering planes), that changed from 0.34 nm of the expanded graphite (Figure 2.6) to about 0.72 nm, meaning that the functional groups present on the oxidized surface and edges, actively help in the separation of the layers, making easier their exfoliation.

In the end, in order to quantify and identify the functional groups present on the graphene

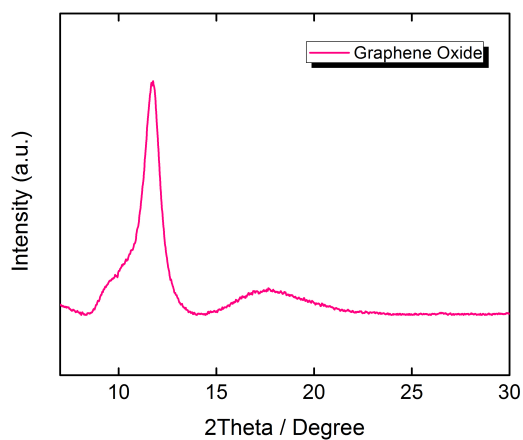


Figure 3.2 XRD data of commercial graphene oxide.

oxide, X-Ray Photoelectron spectroscopy (XPS) analysis was performed, and the result is reported in Figure 3.3. From the analysis of the deconvolution peaks, it was possible to identify the C-C peak at 284.6 eV, the C-O peak at 286.5 eV, the C=O peak at 287.9 eV and the O-C=O peak at 289.1 eV (95). In particular, the intensities of the C-C and C-O peak are really similar confirming the high oxidation state of the graphene oxide.

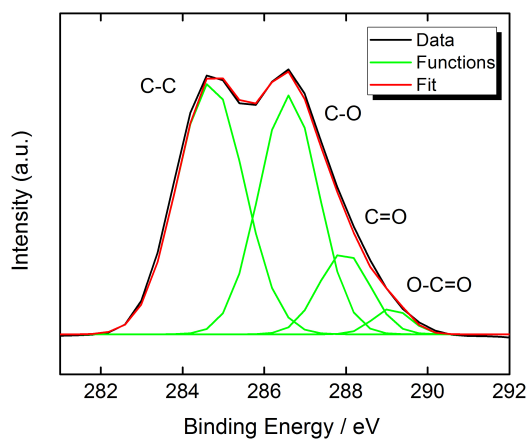


Figure 3.3 XPS data of commercial graphene oxide.

### 3.2.1 Sodium Silicate Catalyzed Graphene Oxide Reduction

The chemical exfoliation of graphite to form individual graphene oxide sheets using strong oxidizing agents has become a most common technique (56). Unfortunately, graphene oxide exhibits poor electronic conductivity due to the interruption of conjugation by substituted oxygen functional groups. Various reducing agents such as  $\text{N}_2\text{H}_4$  (89),  $\text{NaBH}_4$  (96) and alcohols (97) have been used to restore the  $\text{sp}^2$  network of highly conducting graphene. Most of the chemical reducing agents commonly used are hazardous or generate hazardous byproducts and for example by using the hydrazine, the reduced graphene tends to irreversibly agglomerate and convert back to graphite.

The challenge is to identify alternative green approaches that use non-toxic chemicals to produce graphene on a large-scale. It has previously been reported that the deoxygenation of graphene oxide occurs under alkaline conditions (98), (99). Sodium silicate is an abundant material and not expensive to obtain, it is called waterglass or liquid glass and it is used for cements, passive fire protection, etc. As shown in Figure 3.4, it forms from silica and sodium hydroxide and the different ratio of the two components determine the pH of the solution. Generally the sodium silicate produces an alkaline solution and it is glassy, colorless and soluble in water.

In this chapter the results of the chemical reduction process on graphene oxide obtained by

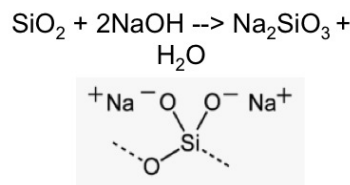


Figure 3.4 Sodium silicate chemical reaction formation and graphic representation of the structure of the structure of the silica gel.

the alkaline action of sodium silicate solutions will be presented.

### 3.2.1.1 Materials and Methods

Only commercial reagents were used: graphene oxide (thickness 0.7–1.2 nm) was purchased from ACS Materials (USA) and used without further purification, sodium metasilicate Mw 122.06 u, citric acid, hydrochloridric acid were purchased from Sigma-Aldrich, deionized water was used as solvent in all the reactions. A solution of 50 mg of sodium metasilicate in 0.5 ml of DI water was obtained by heating it on a hot plate at 80°C for 5 minutes under stirring with a magnetic bar. Dispersions of graphene oxide in DI water were obtained under mild sonication (25 W, 40 kHz) for a total volume of 0.5 ml and a concentration of graphene oxide of 0.5 mg/ml.

The graphene oxide dispersions were then added to the sodium silicate solutions in order to obtain a 1.05 equivalent of the solution of sodium silicate in water, and put on the hot plate at 95°C for 10-15 minutes. The temperature was controlled by the thermostat of the bath sonicator, and the whole vessel was subjected to mild sonication (25 W, 40 kHz). The final suspension was then allowed to cool to room temperature. Intensive centrifugation of the final suspension was performed at 15 000 g for 1 hour, followed by washing with distilled water.

### 3.2.1.2 Results and Discussion

During the preparation of these composites with the graphene has been observed that a stable graphene suspension could be quickly prepared by simply heating an exfoliated-graphene oxide suspension in sodium silicate alkaline solutions at moderate temperatures (50-90°C) and the addition of sodium silicate to the graphene oxide dispersion was accompanied by a fast, unexpected color change, from yellow-brown to homogeneous black (98), (100) and (101).

Several experiments have been performed in order to analyse the actual dependence on the concentration of the sodium silicate and time of exposure to the temperature. Solutions with an increasing amount of sodium silicate, respectively 5, 50, 200 mg were prepared, heated at 180°C for 10 and 60 minutes, as reported in Figure 3.5.

In Figure 3.6 are reported the resulting dispersions of graphene oxide in water and sodium



Concentration of sodium silicate/ mg	temperature/ C	time/ min
/	180	10
		60
5	180	10
		60
50	180	10
		60
200	180	10
		60

Figure 3.5 Table reporting the parameters of the samples of graphene oxide in sodium silicate water solution prepared.

silicate after the heating treatment at 180°C and after adding 10 ml of DI water to reduce the pH of the dispersions, respectively from the left there are the graphene oxide in water without heat treatment, graphene oxide in water heated for 10 min, graphene oxide in water heated for 60 min, graphene oxide with 5 mg sodium silicate heated for 10 min, graphene oxide with 5 mg sodium silicate heated for 60 min, graphene oxide with 50 mg sodium silicate heated for 10 min, graphene oxide with 50 mg sodium silicate heated for 60 min, graphene oxide with 200 mg sodium silicate heated for 10 min and graphene oxide with 200 mg sodium silicate heated for 60 min.

It is very noticeable the difference in color of the samples showing a change from light brown

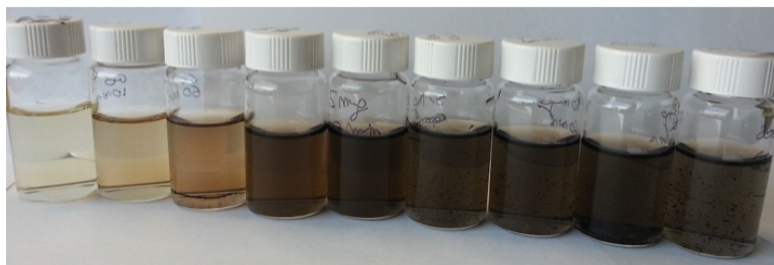


Figure 3.6 Pictures showing the different colors of the samples prepared with different concentration of sodium silicate and heated for different period of time.

to gray/black, meaning that the reduction process occurred by increasing the sodium silicate concentration and the time of heating. The dispersion of reduced graphene oxide in sodium

silicate solution are very homogeneous and stable in time also without the use of surfactant. Careful experiments revealed that exfoliated graphene oxide can undergo fast deoxygenation in strongly alkaline solutions, resulting in stable aqueous graphene suspensions. These phenomena have been previously observed (102) showing how reduced graphene oxide can be stable in solution also without any surfactant agent. It was observed that the electrostatically stabilized dispersion are strong dependent on pH; in fact, the surface of the reduced graphene oxide is charged negatively because of the carboxylic acid and phenolic hydroxyl group that, during the reduction from a neutral charge, became more and more negative, resulting in the retardation of agglomeration of the graphene sheets because of the electrostatic repulsion.

The precipitation of reduced graphene oxide can occur in neutral pH and is mainly due to the less hydrophilic nature due to the removal of oxygen functional groups (103). In Figure 3.7 are reported FE-SEM pictures showing different magnifications of the graphene flakes after the reduction. The size of the flakes is about 10  $\mu\text{m}$  diameter and it is possible to see the typical wrinkles of the graphene sheets.

Free-standing graphene paper samples were also obtained by vacuum filtration, and a picture of a freestanding reduced graphene oxide is shown in Figure 3.8. The thin films obtained by filtration are easily manageable and flexible, and they are ready to be used as electrode for carbon based double layer capacitor devices.

FE-SEM images of the surface and the cross section of the rGO free-standing paper are shown in Figure 3.9. The shape is irregular and individual graphene sheets crumpled enhancing the surface area and a micro porous layered structures is visible at the cross section, that for this particular sample is about 10  $\mu\text{m}$  thick.

X-Ray Diffraction (XRD) characterization was performed to investigate the atomic structure of the reduced sample and compare it with the starting material graphene oxide and the expanded graphite. The spectra reported in Figure 3.10 shown the spectra of expanded graphite (blue), graphene oxide (pink) and reduced graphene oxide with sodium silicate (green). The graphene oxide has a larger layer distance ( $d$ ) compared to the graphite and the reduced graphene because of the functional group present on its surface.

In fact, the graphene oxide diffraction peak shifts to a lower 2 theta angle (11.6) which cor-

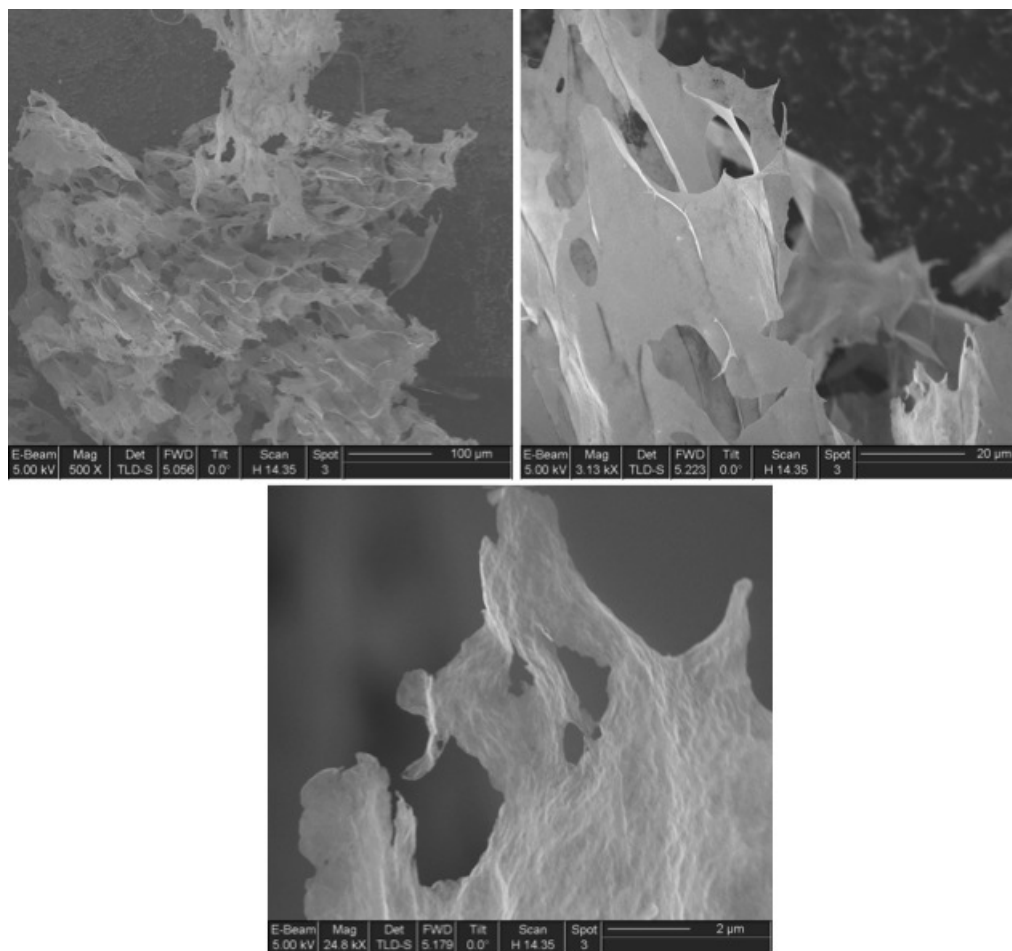


Figure 3.7 FE-SEM pictures of reduced graphene oxide after temperature treatment in sodium silicate solution.

responds to an interlayer distance of approximately 0.72 nm and this indicates the graphene oxide sheets are separated due to the covalently bonded oxygen. The interlayer distance of reduced graphene oxide instead present a peak shifted at 18.2 corresponding to 0.37 nm interlayer spacing. The decrease in interlayer spacing between individual graphene sheets is attributed to the Van der Waals interactions between  $sp^2$  hybridized carbon frame-work that is restored during the chemical reduction.

The peak of the reduced graphene oxide is larger and broader than the one of the graphite because of the structural defects introduced by the processing and the sonication (98), (100) and (101).

The deoxygenation of graphene oxide was also analyzed by X-ray photoelectron spectroscopy



Figure 3.8 Picture of a freestanding rGO easily manageable flexible paper on an alumina filter for vacuum filtration.

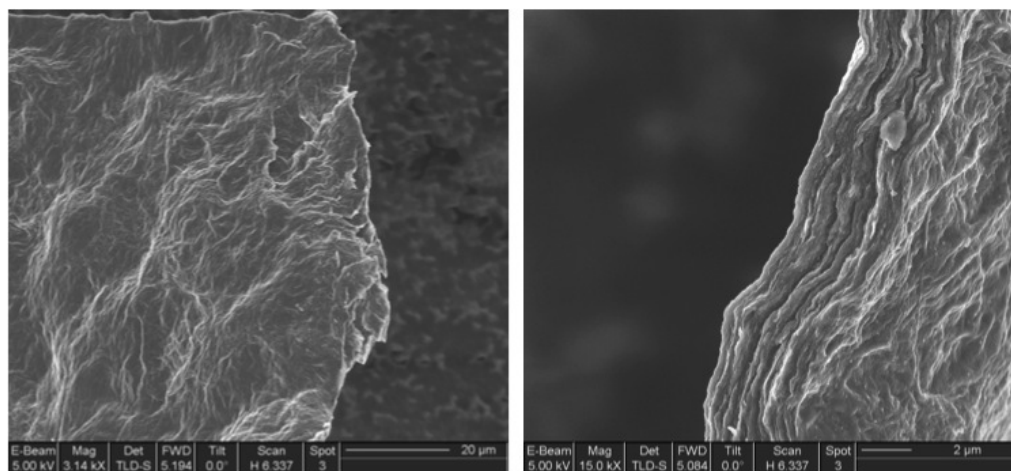


Figure 3.9 FE-SEM pictures of the top view and cross section of the layered reduced graphene paper obtained after vacuum filtration.

(XPS) to reveal the intensity of the carbon functional groups. The reduction of the oxygen functional groups after the process with the sodium silicate is reported in Figure 3.11, where the deconvolution peak of the C1s is compared with the starting material. From the survey it is also possible to see that the reduced graphene oxide shows the presence of the sodium peak Na KLL as reported in Table 3.1, due to a residue of the sodium of the sodium silicate not completely removed washing the sample; in particular, it is higher in the sample reduced using an higher concentration of sodium silicate.

After the reduction in sodium silicate solution the peaks O-C=O at 289 eV, C-O at 286.4 eV

Table 3.1 Survey atomic percentage of C 1s and Na KLL.

Sample	C 1s	Na KLL
Graphene oxide	98.5	0.1
Low concentration	84.3	3.2
High concentration	88.1	9.9

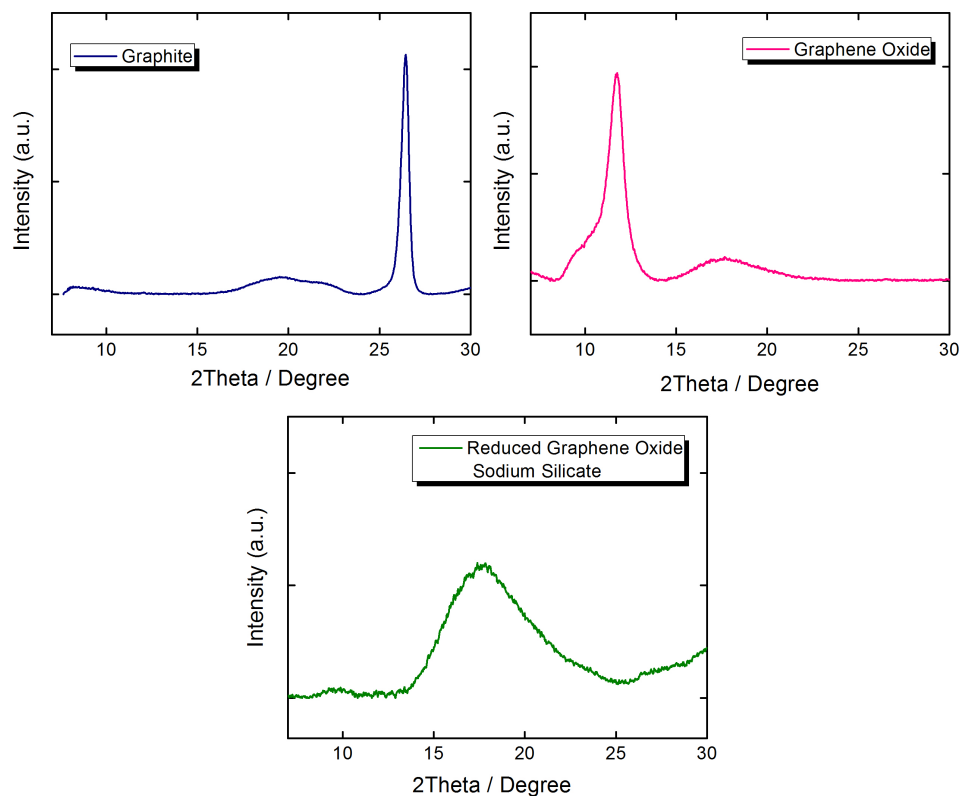


Figure 3.10 X-Ray Diffraction spectra of expanded graphite (blue), graphene oxide (pink) and reduced graphene oxide with sodium silicate (green).

and C=O at 287.8 eV have reduced their intensities compared to the graphene oxide C1s XPS spectrum. The deconvoluted XPS spectra of the C1s for rGO show in particular a dramatic decrease in the intensity of C-O species due to the reduction of sodium silicate (98), (100) and (101).

**Comparison with NaOH** In order to compare the effects of the reduction throughout the use of sodium silicate ( $\text{Na}_2\text{SiO}_3$ ) and sodium hydroxide (NaOH), an experiment was conducted by preparing three dispersions of graphene oxide in DI water with a concentration of 1 mg/ml and other two with respectively 1M  $\text{Na}_2\text{SiO}_3$  and 1M NaOH for a total volume of 2 ml.

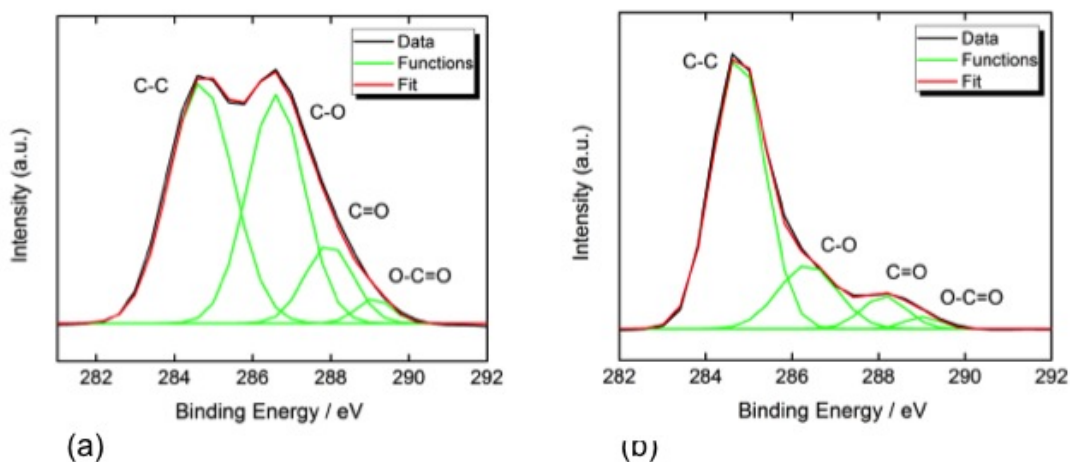


Figure 3.11 X-Ray Photoelectron Spectroscopy spectra of a) Graphene oxide and b) reduced graphene oxide.

In Table 3.2 is reported the temperature for the reactions, that was maintained at 80°C for 35 minutes.

The dispersions of GO in water with 1M of  $\text{Na}_2\text{SiO}_3$  and 1M NaOH before and after the

Table 3.2 Samples concentrations, temperature and time of the reduction process.

Sample	Concentrations (M)	Temperature (C)	Time (minutes)
$\text{Na}_2\text{SiO}_3$	1	80	35
NaOH	1	80	35

reduction process are showed in Figure 3.12. It is possible to notice that the reaction with

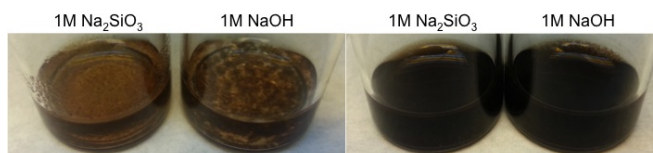


Figure 3.12 Pictures of the dispersions of GO in water with 1M of  $\text{Na}_2\text{SiO}_3$  and 1M NaOH before and after the reduction reaction.

the NaOH starts right after when it gets in contact with the graphene oxide, and areas of higher concentration of graphene are formed. When the reduction process is completed, it is almost impossible to distinguish the two samples by the color, that has become from light brown, to a

very dark brown/black. In Figure 3.13 the two final dispersions of reduced graphene oxide are compared with a dispersion of graphene oxide in water with the same concentration after the same thermal treatment. It is possible to notice from the difference in color, that the thermal treatment itself is not enough to produce the same reduction in the graphene oxide.

In order to obtain quantitative information on the reduction differences using sodium silicate

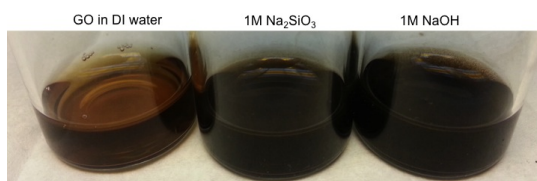


Figure 3.13 Pictures of the dispersions of GO in water compared to dispersion with 1M of  $\text{Na}_2\text{SiO}_3$  and 1M NaOH after thermal treatment.

and NaOH, another experiment was conducted. In this case, dispersions of graphene oxide in DI water with a concentration of 1 mg/ml and other two with respectively 1 M sodium silicate 8M NaOH and 1M NaOH for a total volume of 18 ml were prepared. In Table 3.3 is reported the temperature for the reaction fixed at  $60^\circ\text{C}$  and the time of reaction was fixed at 180 minutes.

In Figure 3.14 are shown four dispersions, respectively of GO in water, GO/8M NaOH, GO/1M

Table 3.3 Samples concentrations, temperature and time of the reduction process.

Sample	Concentrations (M)	Temperature (C)	Time (minutes)
$\text{Na}_2\text{SiO}_3$	1	60	180
NaOH	8	60	180
NaOH	1	60	180

of  $\text{Na}_2\text{SiO}_3$  and GO/1M NaOH in DI water after the reduction reaction, and from the dark color of the dispersion is possible to see that a reduction of the graphene oxide has occurred.

In order to confirm and to quantify the reduction degree at these four samples XPS analysis was performed, and C1s spectra are reported in Figure 3.25. From the values of the C/O ratio reported in Table 3.4, it is possible to see that the intensity of the deconvolution peak of the functional group C-O compared to the one of the graphene oxide result decreased for all three samples, while the C=O group shows a decrease in the intensity only for the sample with

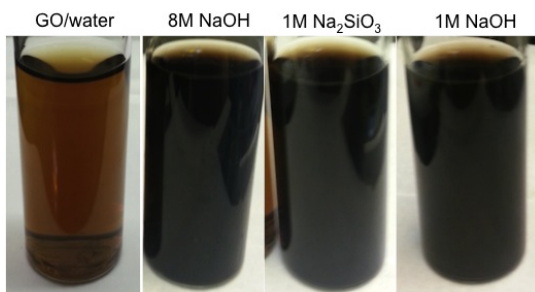


Figure 3.14 Pictures of the dispersions of GO in water and GO/1M of Na<sub>2</sub>SiO<sub>3</sub>, GO/8M NaOH and GO/1M NaOH after the reduction reaction.

1M NaOH.

In the end it is possible to conclude that the reduction of the graphene oxide through the

Table 3.4 Ratio C/O of carbonyl and carboxyl group of GO, GO/8M NaOH, GO/1M of Na<sub>2</sub>SiO<sub>3</sub> and GO/1M NaOH samples.

Sample	Carbonyl group C=O	Carboxyl group O-C=O
GO	0.71	5.11
Na <sub>2</sub> SiO <sub>3</sub>	2.55	4.82
1M NaOH	2.98	5.59
8M NaOH	3.72	3.77

use of Na<sub>2</sub>SiO<sub>3</sub> water based solutions was proved and that the suspensions obtained show a long-term stability (months instead of few hours, if compared with dispersions of graphene in other solvent, like NMP). It was also confirmed that the mechanism of reduction depends on the NaOH concentration and that higher pH correspond to higher reduction degree, as confirmed by the sample with 8M NaOH. 1M NaOH and 1M Na<sub>2</sub>SiO<sub>3</sub> are quite comparable for the C/O ratio values and has been observed an improvement in the reduction of the carboxyl group for the Na<sub>2</sub>SiO<sub>3</sub> sample, compared to the 8M NaOH.



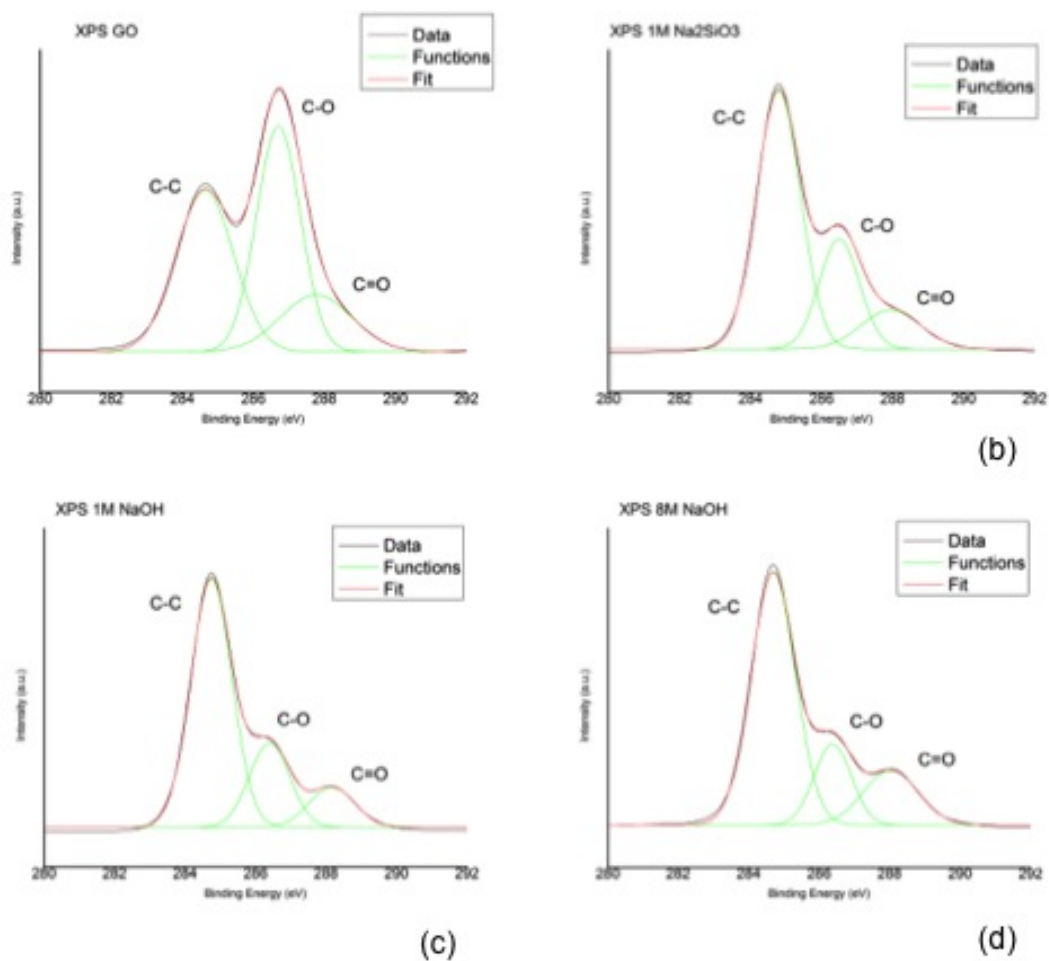


Figure 3.15 X-Ray Photoelectron Spectroscopy spectra of a) Graphene oxide and b) reduced graphene oxide with 1M of Na<sub>2</sub>SiO<sub>3</sub>, c) 1M NaOH and d) 8M NaOH.

### 3.2.2 UV-light Catalyzed Graphene Oxide Reduction

The possibility of reducing GO by irradiation with UV light can be exploited. In the next sections are reported the results of the reduction of GO, performed using UV light irradiation. The addition of photo initiating molecules and their role in the speeding up of the reduction process due to the formation of free radicals (111) will be also discussed.

The UV curing process can be used to concurrently achieve the polymerization of the acrylic matrix and the reduction of the GO filler (112) and the detail of the procedure followed for the fabrication and the characterization of an environmentally friendly printable ink, starting from water-based stable dispersions of GO and subsequent addition of the polymeric matrix will be presented in chapter 4 (111).

#### 3.2.2.1 Materials and Methods

Only commercial reagents were used: graphene oxide powder was purchased from Cheap Tubes Inc. (USA) and DAROCUR 1173 radical photo initiator (PI) from BASF. All reagents were used without further purification and deionized water was used as solvent in all the reactions.

Spin-coated GO aqueous dispersions were prepared by mixing GO powder and PI in 1 g of deionized water. The GO concentration in water was varied between 1 and 4 per hundred parts of resin (phr), while the PI content was varied between 1 and 8 phr. The relative GO/PI content was varied between 1/0.25 and 1/8 weight ratio, to evaluate the PI content effect on the GO reduction. The GO aqueous dispersions were spin-coated on 1 cm<sup>2</sup> portions of single crystalline p-doped silicon wafer, pre-cleaned by ultrasonic bath in isopropyl alcohol, rinsed with water, and dried with nitrogen. The coated formulations were irradiated with UV light for 2 min, with a light intensity of 60 mW/cm<sup>2</sup>. After UV irradiation, samples were dried at 80°C under vacuum for 2 hours to remove residual water.

**Inkjet printed GO aqueous dispersions** A printable GO/water dispersion was formulated by mixing 0.02 g of GO powder in 4.5 g of deionized water. In this formulation, a lower concentration of GO was used to reduce the viscosity to a value compatible with the use of the inkjet nozzle. High-speed Ultraturrax was used for 5 min to obtain a homogeneous dispersion. Two-step ultrasonic bath (30 min at 40 kHz and 30 min at 59 kHz) was then used to further grind and disperse the GO agglomerates. Finally, the dispersion was centrifuged at 14,000 rpm for 5 min to allow residual large and heavy particles to precipitate at the bottom of the test tube.

The upper portion of the centrifuged dispersion was inserted into an ink reservoir, thus discarding the large precipitated particles. The graphene water based ink was tested with an Inkjet Printing System (Jetlab-4XL from MicroFab, US) with automatic 3D position control, using an 80  $\mu\text{m}$  orifice piezoelectric nozzle vibrating at a frequency of 250 Hz, at room temperature. A test pattern of the GOi formulation (prepared to assess the system printability) was printed on a Si substrate for structural characterization.

GO aqueous dispersions with a concentration of 4 mg/ml were prepared by mixing GO powder and PI in deionized water, with a relative concentration GO/PI equal to 1/4, using high-speed Ultraturrax to obtain a homogeneous dispersion, followed by ultrasonic bath to further grind and disperse GO agglomerates.

The bipolar asymmetrical pulse is normally preferred to facilitate droplet formation and ejection (a more detailed explanation of the printing parameters is reported in chapter 4).

Straight line patterns were printed on glass slides and several values of resolution and thickness were tested. The dimension and speed of ink drops were controlled using a horizontal camera located onto the xy stage for direct drop observation. Using the described printing setup, ink drops with a diameter of 100  $\mu\text{m}$  were normally obtained. Since resolution is not an issue, in this study devoted to the characterization of the UV-induced reduction, we did not optimize the ejection parameters, which normally enable a printing resolution beyond 50  $\mu\text{m}$ . A drop spacing of 200  $\mu\text{m}$  was used to achieve complete coverage of the patterned substrate.

### 3.2.2.2 Results and Discussion

Darocur 1173 is generally employed as additive to initiate the polymerization process to cross-link the starting material through UV curing processes and its chemical structure is shown in Figure 3.16.

The dispersion of graphene oxide in water obtained after the sonication process and the ad-

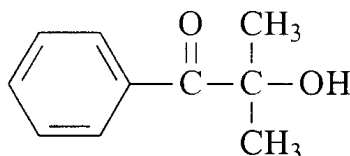


Figure 3.16 Darocur 1173

dition of the photo initiator was printed on different substrate as silicon wafer or glass slides as shown in Figure 3.17, and the printed tracks showed a good uniformity and coverage of the substrate as shown in Figure 4.10, where tracks with different thickness are shown, corresponding to variation of dpi resolution or several repetition of the printing. After the printing



Figure 3.17 Image showing inkjet print head, printing on a glass slide.

step, the tracks were irradiated under a Hg-lamp UV-light (Figure 3.18) with an intensity of  $55 \text{ mW/cm}^2$  for 2 minutes.

Several test patterns of the GO/water/PI ink formulations were inkjet printed on transparent substrates (microscope glass slides) as shown in Figure 3.19, where are shown straight lines of the GO/PEGDA formulation with various thicknesses. In order to confirm the effectiveness of GO reduction by UV irradiation, XPS spectra of samples deposited on Si wafer were compared before and after irradiation. The GO/PI weight ratio was varied from 1/0.25 to 1/8 (S1

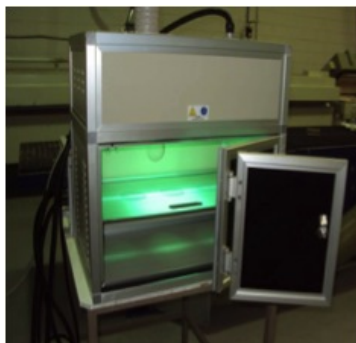


Figure 3.18 Hg-lamp, UV-light with intensity 55 mW/cm<sup>2</sup>

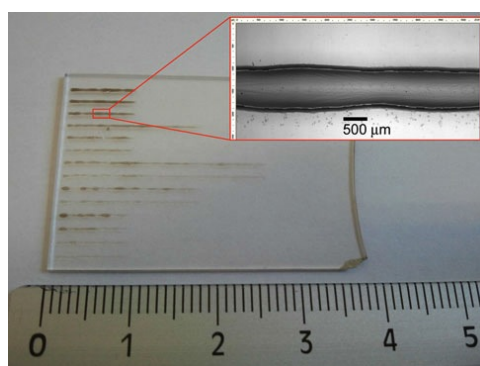


Figure 3.19 Image showing inkjet printed test tracks of the GO ink on a microscope glass, after UV irradiation.

= 1/0.25; S2 = 1/0.5; S3 = 1/1; S4 = 1/2; S5 = 1/4; S6 = 1/8 wt ratio). Figure 3.25 reports an example of the variation of XPS C1 s peaks after 2 min of UV irradiation of an aqueous dispersion containing 1 phr of GO and 4 phr of PI with respect to water, showing the best fits (red) to experimental data (black) and the deconvoluted peaks (blue) used for fitting. The spectrum in (b) refers to the formulation containing a GO/PI ratio of 1/4.

After irradiation, it is possible to observe a significant decrease in intensity of the peaks associated with carbonyl groups, evidencing the photoinduced GO reduction (113). This deconvolution evaluation was performed on different aqueous GO dispersions varying both GO and PI content, to evaluate the best performing GO/PI ratio. The area and height of XPS peaks associated with carbon-carbon and carbon-oxygen bonding (carbonyl and carboxyl groups) have been analyzed.

Figure 3.21 summarizes the analysis of the ratios of heights and areas of peaks associated with

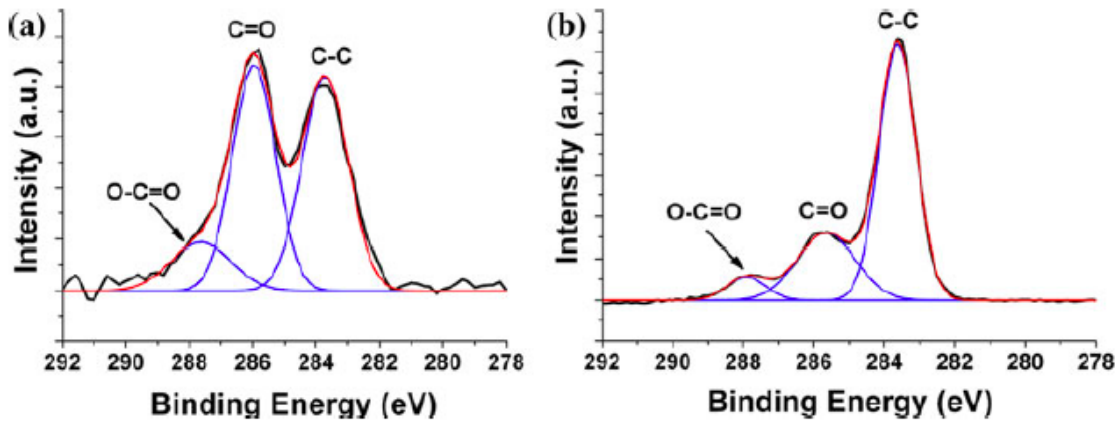


Figure 3.20 XPS spectra of pristine GO (a) and a sample irradiated for 2 min with UV light (b)

carbon–oxygen and carbon–carbon groups, proving that all samples show a decrease of oxygen bonded to carbon after UV irradiation, for samples with several concentrations of GO and PI in water after 2 min of UV irradiation (the formulations correspond to the GO/PI ratio reported as following: S1 = 1/0.25; S2 = 1/0.5; S3 = 1/1; S4 = 1/2; S5 = 1/4; S6 = 1/8 wt ratio). For comparison, pristine GO before UV irradiation is also reported.

The measurements prove the reduction of GO, with restoration of the extended conjugated sp<sup>2</sup> structure. According to these results, the sample with GO/PI ratio of 1/4 gave the highest value of GO reduction. In chapter 4 of this dissertation will be explored the possibility of using this reduction technique for the formulations of graphene composites, using graphene oxide as a conductive filler for insulating photocurable resins and their application as inks for flexible printed electronics.

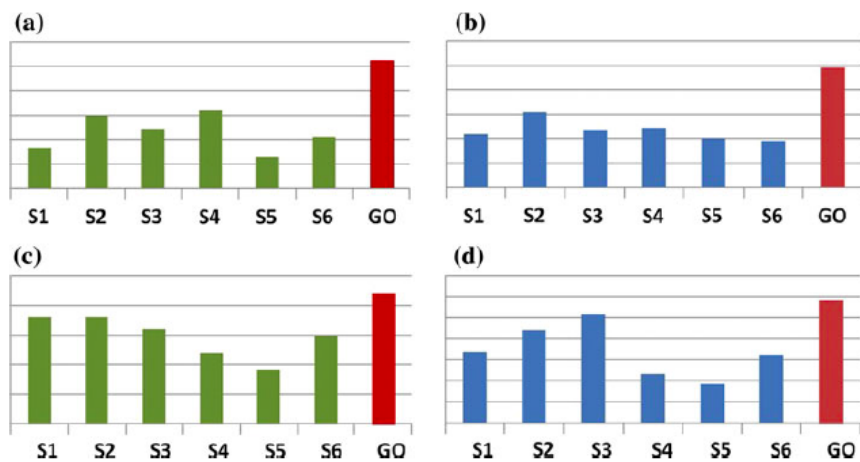


Figure 3.21 Analysis of XPS C1s peak deconvolution: height (a) and area (b) ratios of C=O to C-C contributions plus height (c) and area (d) ratios of O-C=O to C-C contributions.

### 3.2.3 Hydrothermal Graphene Oxide Reduction

Self-assembly is one of the most effective strategies for bottom-up nanotechnology and in this next section the result of the synthesis of self-assembling 2D graphene sheets into complex three-dimensional (3D) macrostructures and the simultaneous reduction of the graphene oxide in reduced graphene oxide by the use of hydrothermal synthesis are presented.

#### 3.2.3.1 Materials and Methods

Only commercial reagents were used: graphene oxide powder was purchased from ACS Materials (USA) and used without further purification, deionized water was used as solvent in all the reactions. Graphene oxide can be readily dispersed in water and dispersions with 12 ml volume and a concentration of graphene oxide of 2 mg/ml were prepared using of a mild sonication (25 W, 40 kHz) for 30 minutes. The GO/water dispersion was then transferred in a 18 ml volume Teflon-lined autoclave (Figure 3.22) and heated in a oven at 180°C for 12 hours. After the hydrothermal process the sample was removed from the autoclave, frozen in liquid nitrogen and dried under vacuum overnight.



Figure 3.22 Picture of the Teflon-lined autoclave used for the hydrothermal synthesis.

#### 3.2.3.2 Results and Discussion

Homogeneous graphene oxide aqueous dispersions were obtained after the sonication process, with a yellow/brown uniform and clear color as shown in Figure 3.23 a. After the hy-